7th ECCOMAS Thematic Conference on Smart Structures and Materials
SMART 2015
A.L. Araújo, C.A. Mota Soares, et al. (Editors)
© IDMEC 2015

A PROCEDURE TO EVALUATE RELIABILITY OF MEASUREMENTS IN A SMART STRUCTURE

Gabriele Cazzulani[*], Simone Cinquemani[*], Marco Ronchi[*], Francesco Braghin[*]

[*]Politecnico di Milano, Dept. of Mechanical Engineering
Via La Masa 1, 20156 Milano (Italy)
simone.cinquemani@polimi.it

Key words: Smart structures, Fiber Bragg Grating, sensor fault, control algorithm.

Summary: *Fiber optic strain sensors, such as Fiber Bragg Gratings (FBG), have a great potential in the use in smart structures thanks to their small transversal size and the possibility to make an array of many sensors. They can be embedded in carbon fiber structures and their effect on the structure is nearly negligible. This paper introduces the use of these sensors to increase the reliability of feedback measurements in smart structures designed to actively control vibrations. As known, one of the main drawbacks of these structures is the robustness of the control when one or more sensors do not work properly. In these cases the performance in reducing vibration can be seriously limited and problems of instability may occur. The use of FBG sensors can overcome this limit thanks to the large number of available measurements. This paper introduces some different control algorithms to suppress vibration and discusses the reliability of feedback measurements when failures on sensors happened. Theoretical results are supported by experimental tests on a large flexible system made of a thin cantilever beam with 14 longitudinal FBG sensors and three piezoelectric actuators (PZT).*

1 INTRODUCTION

Centralized control logics are based on a single controller which gets information from a certain number of sensors and generates consequently a certain number of control forces. Among the different sensors that can be used for vibration control, this paper focuses on Fiber Bragg Grating sensors. Indeed, these sensors, mostly used for structural health monitoring [1,2], in the last years have been considered in different vibration control applications[3-5]. The reason of this development is that these sensors have some significant advantages with respect to traditional ones, such as the reduced size, which implies a very low load effect and the possibility to embed them into the structure, and the possibility to embed a large number of sensors on a single fiber, thus reducing the wiring complexity [6]. On the contrary, they have some problems which have to be carefully addressed [7]. In particular, as shown in [8], the embedding process can introduce larger measurement uncertainties, reducing the quality of the sensor output.

Typically, when defining the control logic and when calculating the control gains, the effect of possible actuator or sensor faults is not taken into account. Consequently, this effect

is unpredictable and it can result in strong reduction of control performance or even in the instability of the controlled system. This paper focuses on the study of the effect of sensor fault when large sensor arrays (such as Fiber Bragg Grating arrays) are considered. Indeed, sensor arrays provide a distributed measurement of the structure vibrations, allowing the design of optimized control logics. Anyway, due to the large number of sensors, the reliability is lower and the malfunctioning of one or more sensors can occur. For this reason, this paper proposes a method to identify the fault or malfunctioning of a sensor and applies this method on a smart structure equipped with an array of FBG sensors. Different sensor problems are simulated to verify the reliability of the proposed solution and the case of multiple sensor fault is also considered.

In order to present the proposed solution and the results obtained, the paper is structured as follows. Section 2 recalls the working principle of FBG sensors, showing the most important characteristics associated to vibration control. Section 3 illustrates the method used for the identification of sensor fault. Section 4 describes the structure used to test the method and its corresponding numerical model, while section 5 shows some numerical results demonstrating the efficiency of the proposed solution.

2 FBG WORKING PRINCIPLE

Fiber Bragg Grating sensors, and more in general optical strain gauges, are a promising technology for active vibration control. The working principle of these sensors is known and deeply described in literature [1], so as the different techniques available to measure the peak shift of the reflected light wave. For the sake of completeness, this section briefly recall how these sensors work. Figure 1 shows the FBG working principle: the light is sent into the fiber from a light source and each sensor reflects it only in a limited range of wavelengths. The spectrum peak of the reflected wavelength is a function of the deformation of the FBG sensor, so measuring the peak it is possible to obtain a measurement of the deformation.

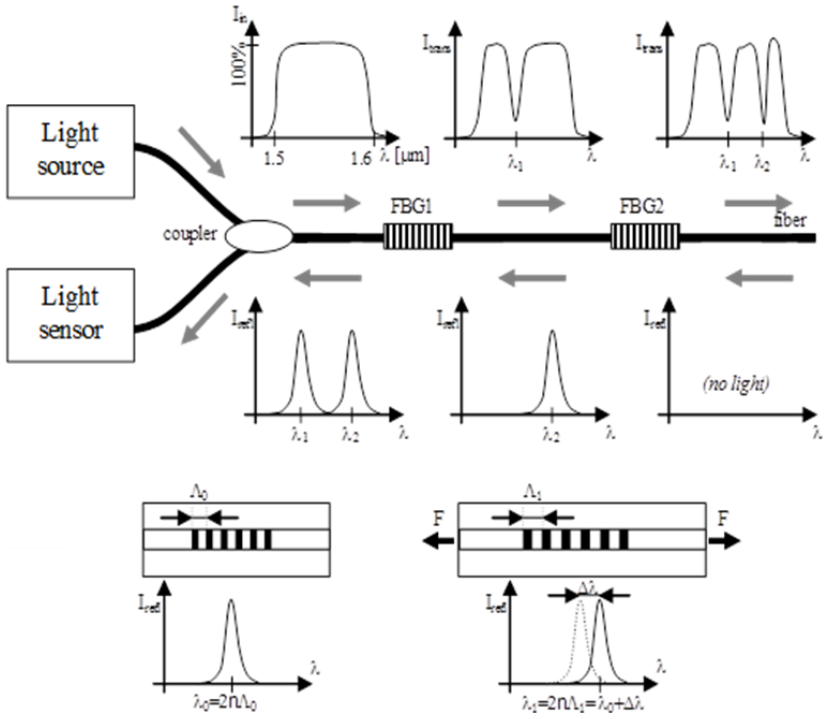

Figure 1: FBG sensors: working principle of a fiber equipping multiple sensors.

The use of Fiber Bragg Grating sensors in active vibration control can be advantageous thanks to their small cross-section that allows to embed these sensors in carbon fiber structures with negligible load effects and to the possibility to embed tens of sensors on the same optical fiber, thus having a large number of measurements without a high number of cables and complex wiring. All hese aspects are interesting in applications of vibration control since these sensors provide an insight into the state of deformation of the structure using a non-invasive measurement system.

In this paper, signals coming from FBG sensors are acquired using a commercial interrogator based on the Swept laser interrogation technique. The adopted interrogator is the MicronOptics SM130-500. It has a resolution of 1 pm and a sampling frequency of 1 kHz, it has four optical channels and it manages a maximum number of 80 FBG sensors on a single channel. The output is provided through a digital TCP/IP Ethernet transmission. This method, if compared with other interrogation techniques, allows managing a larger number of sensors and provides a higher flexibility to sensors characteristics (e.g. the wavelength). This allows extending the results obtained in this work to a large number of practical applications and sensor configurations.

Despite the advantages of this technology are evident, there are a number of limitations to its use in applications of vibration suppression undermining the effectiveness of control. In particular, it has been shown that the quality of the measurement of the single sensor can be strongly affected by the embedding process. As a consequence, different sensors on the same fiber can measure the deformation signal with different precision. Moreover, considering a more general case involving more than one fiber, sensor faults can occur on some of the sensors used for the feedback control.

For these reasons, the identification of the sensor faults is a key point for the reliability of the control system based on these sensors. The following section will present a method for the sensor fault identification.

3 THE ALGORITHM FOR THE IDENTIFICATION OF SENSOR FAULTS

Considering the dynamic equation of a generic mechanical system, it is known that the measurements $\mathbf{Y}$ can be decomposed into their principal (or modal) components by

$$\mathbf{Y} = \mathbf{\Phi q} \tag{1}$$

where $\mathbf{q}$ is the vector containing the modal coordinates and $\mathbf{\Phi}$ contains the system modes evaluated at the points of application of the sensors. Assuming that all the sensors work correctly, an estimator of the measurements can be defined as

$$\hat{\mathbf{Y}}^0 = \mathbf{\Phi}\mathbf{\Phi}^*\mathbf{Y} \tag{2}$$

where the symbol * is used to identify the Moore-Penrose pseudo-inverse matrix.

On the contrary, if one or more sensors are faulty, the estimator defined in (2) do not provide a correct measurement estimation, due to the unwanted effect of non-working sensors. For this reason, in order to compute a new correct estimator, the measurement vector $\mathbf{Y}$, together with the estimation and the modal matrix, can be partitioned into faulty (k) and non-faulty ($\bar{k}$) sensors

$$\mathbf{Y} = \begin{bmatrix} \mathbf{Y}^k \\ \mathbf{Y}^{\bar{k}} \end{bmatrix} \qquad \hat{\mathbf{Y}}^0 = \begin{bmatrix} \hat{\mathbf{Y}}^{0(k)} \\ \hat{\mathbf{Y}}^{0(\bar{k})} \end{bmatrix} \qquad \mathbf{\Phi} = \begin{bmatrix} \mathbf{\Phi}^k \\ \mathbf{\Phi}^{\bar{k}} \end{bmatrix} \tag{3}$$

Similarly to equation (2), the measurement estimation can be performed, considering only the working sensors and the corresponding modal matrix partition, as

$$\hat{\mathbf{Y}}^{\bar{k}} = \boldsymbol{\Phi}^{\bar{k}} \left(\boldsymbol{\Phi}^{\bar{k}} \right)^{*} \mathbf{Y}^{\bar{k}} \tag{4}$$

The quality of the measurement estimations and the difference between the estimation resulting from equations (2) and (4) are directly connected to the presence of faulty sensors. To quantify these differences, different residuals can be used. The most common ones are defined as

$$\begin{aligned} \boldsymbol{\gamma}_k^0 &= \hat{\mathbf{Y}}^{0(\bar{k})} - \mathbf{Y}^{\bar{k}} \\ \boldsymbol{\gamma}_k &= \hat{\mathbf{Y}}^{\bar{k}} - \mathbf{Y}^{\bar{k}} \end{aligned} \tag{5}$$

As shown in [9], a new residual can be introduced. Indeed, it has been shown that this new residual is robust to measurement noise and it has better properties of fault detection, which is the scope of the paper. This new residual is defined as the difference between the two residuals shown in (5)

$$\boldsymbol{\zeta}_k = \boldsymbol{\gamma}_k^0 - \boldsymbol{\gamma}_k = \hat{\mathbf{Y}}^{0(\bar{k})} - \hat{\mathbf{Y}}^{\bar{k}} \tag{6}$$

When no faults are present in the measurement system, all the residuals are close to zero, since the estimation of the modal coordinates (and, as a consequence, the estimated measurements) is good and the estimation error is negligible. On the contrary, if a faulty sensor is present, two cases can be distinguished:

- sensor k is the faulty one: in this case, the residual $\boldsymbol{\gamma}_k$ is close to zero, since it is calculated excluding the faulty sensor, while the residual $\boldsymbol{\gamma}_k^0$ is different from zero;
- sensor k is not the faulty one: both the residuals $\boldsymbol{\gamma}_k$ and $\boldsymbol{\gamma}_k^0$ are different from zero, because they are computed using the information of the faulty sensor.

So in the presence of a fault, the residual $\boldsymbol{\zeta}_k$ increases, being the difference of the two. It is demonstrated [9,10] that the sensor corresponding to a faulty condition can be identified by computing the correlation index, defined as

$$\rho_k = \frac{E\left[\boldsymbol{\zeta}_k^T \boldsymbol{\gamma}_k^0 \right]}{\sqrt{E\left[\left\| \boldsymbol{\zeta}_k \right\|^2 \right]}} \tag{7}$$

for all the sensors of the structure (k=1,.....,n, where n is the number of sensors). the faulty sensor corresponds to the highest correlation index.

4 THE NUMERICAL AND EXPERIMENTAL ANALYSIS

The algorithm for sensor fault identification presented in the previous section has been tested numerically and experimentally on a smart structure and its numerical model. In the following (section 4.1), the structure will be described together with the numerical model. Then (section 4.2), the main results obtained will be presented and discussed.

4.1 The structure

The test rig (figure 2) is a clamped-free beam equipped with an array of FBG sensors [7].

Its dimensions are 850 mm × 105 mm × 1.7 mm and it is made by three layers of unidirectional carbon fiber. A chain of 14 FBG sensors placed on a single optical fiber has been selected. Each sensor has a grating length of 8 mm and all the sensors are equally spaced both in distance (60 mm) and in wavelength (4.7 nm, from 1515 nm to 1576 nm). Three piezoelectric actuators have been bonded to the structure, co-located with sensors 3,7,and 10 respectively. These actuators, used to excite the structure, are QP20W produced by Midé.

Figure 2: A picture of the test rig.

The large number of available measurement points is a great potential which, to be fully exploited, needs a numerical model describing the dynamics of the system. The system is discretized with a Finite Element Method (FEM) mesh of 36 nodes. Each node, except for the first one, which is fixed to the ground, can translate and rotate in the plane. The deformation sensed by the FBG sensors is approximated with the difference of rotation between two adjacent nodes, placed at the ends of the sensor itself. Similarly, PZT actuators are modeled as two torques applied on the nodes placed at the ends of the devices. Figure 3 shows the comparison between analytical, numerical and experimental modal curvatures of the first two modes along the beam. The vertical axes represent the curvature of each modal shape, normalized so that the modal curvature on the second FBG sensor is equal to 1. The horizontal axes, whose ticks are the sensors' number (from 1 to 14) represents the beam length. Sensor 1 is the sensor closest to the clamp, while sensor 14 is close to the beam tip. The analytical model has uniform characteristics along the structure and then does not include the local stiffening effect due to the actuators. On the contrary the finite element model is more detailed and includes this effect. A good match between numerical and experimental modes can be observed. As the local stiffening effect introduced by the PZT patches is well represented by the numerical model. For this reason, in the following section,

the numerical results will be presented. Due to the good match between the model and the real system, all the results obtained can be easily extended to the practical situation.

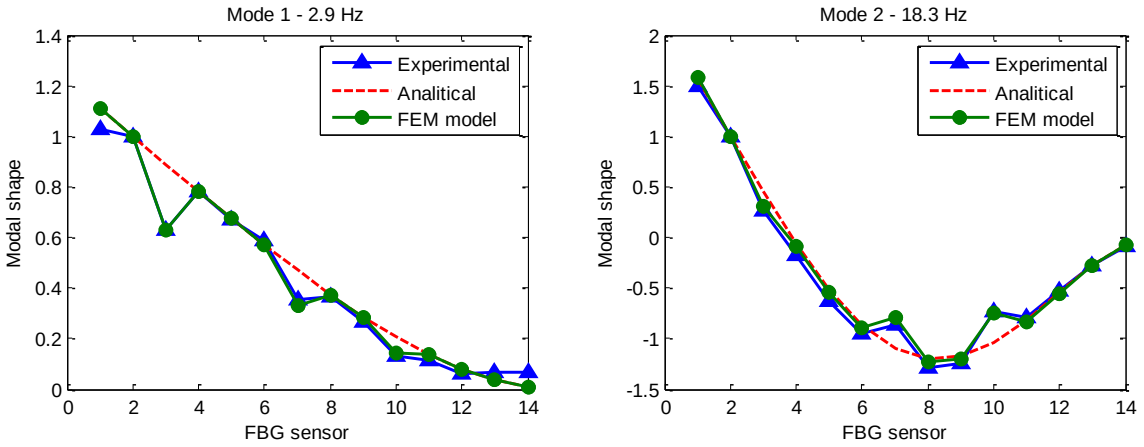

Figure 3: Comparison between the experimental mode and the numerical and analytical ones. First mode (on the left) and second mode (on the right).

4.2 Results and discussion

The fault identification logic presented in section 3 has been tested on the smart structure described in section 4.1 to verify its effectiveness in identifying the sensor faults. In order to consider a particularly critical condition (multiple sensor faults at the same time) and to analyze different sensor problems, the following sensor faults have been simulated by modifying the measurement:

- *Sensor 2 and sensor 13*: measurement equal to zero (it simulates the presence of a switched-off sensor);
- *Sensor 4 and sensor 10*: high random noise summed to the measurement (it simulates the effect of sensors affected by high measurement noise due to external disturbances or noise sources);
- *Sensor 7*: the measurement is one half of the correct one (it simulates the effect of a reduced sensitivity of the sensor due, for example to a partial fault of the connection between the sensor and the structure, or the effect of a sensor with wrong calibration).

Considering this working condition, different tests have been carried out, exciting the structure in different ways in order to simulate the most typical working condition of the measurement system. Among all the experiments, for the sake of brevity, this paper reports two significant tests.

The first test has been performed by exciting the structure with a harmonic disturbance at its first resonance frequency (2.9 Hz). Figure 4-a shows the correlation index for each sensor. It can be seen that the index referred to sensor 2 is strongly higher than the other ones, which means that sensor 2 is faulty. Once identified sensor 2 as faulty, the same procedure is repeated excluding it from the calculation (figure 4-b). Generalizing, each figure (iteration) is realized excluding from the computation all the sensors identified as faulty in the previous figures (iterations). For each iteration, the sensor with a higher correlation index is the one identified as faulty and excluded. Anyway, a sensor is considered as faulty only if the ratio between its correlation index and the higher one among the other sensors is greater than 1.5. This means that the residuals associated to the assumption that the sensor is faulty are

significantly lower than the ones including the sensor.

Summarizing, the algorithm correctly identifies as faulty sensors 2, 4 7 and 10. It can be seen that the fault of sensor 13 is not identified. This can be explained since sensor 13 is close to the free end of the beam, which correspond to a node for any deformation mode (see figure 3). Consequently its measurement signal is very low and its contribution on the modal coordinate estimation is negligible.

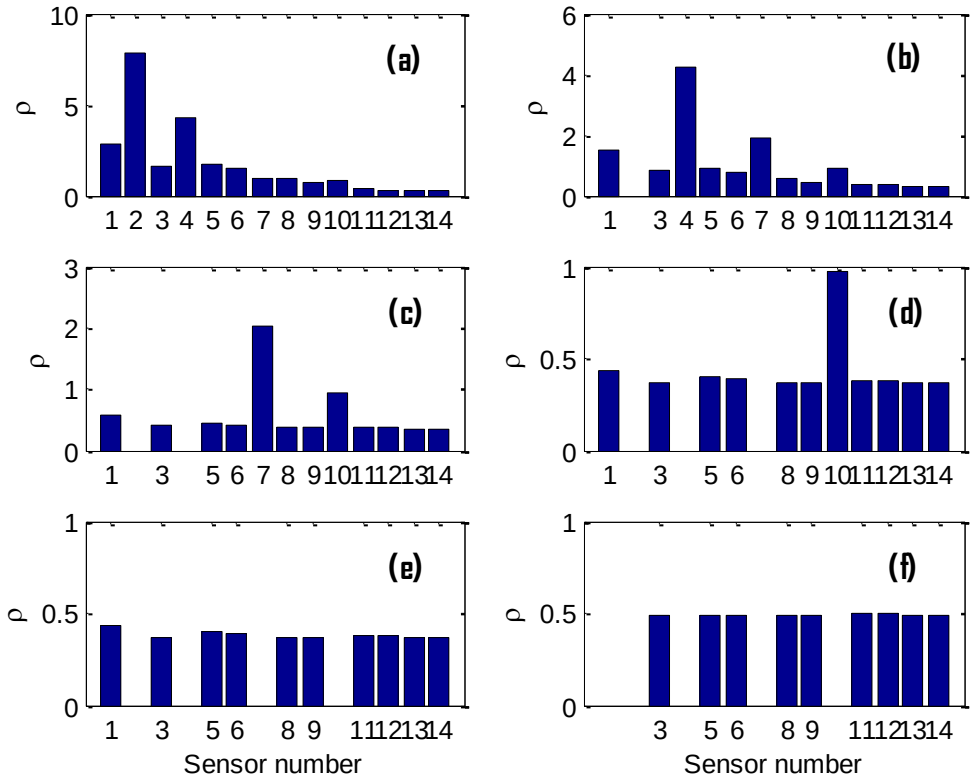

Figure 4: Sinusoidal disturbance on the first natural frequency: correlation index for the different sensors. Each figure is computed excluding the sensor identified as faulty in the previous iteration.

Figure 5 shows the estimation of the first modal coordinate of the structure, comparing the result considering all the sensors and the result excluding the sensors identified as faulty (2,4,7,10). The estimation considering all the sensors shows a significant error with respect to the exact value. On the contrary, the proposed solution allows identifying the faulty sensors and obtaining a prefect estimation. To confirm this statement in a more quantitative way, table 1 shows the root mean square (RMS) value of the estimation error for the first three modes before and after the application of the fault identification method.

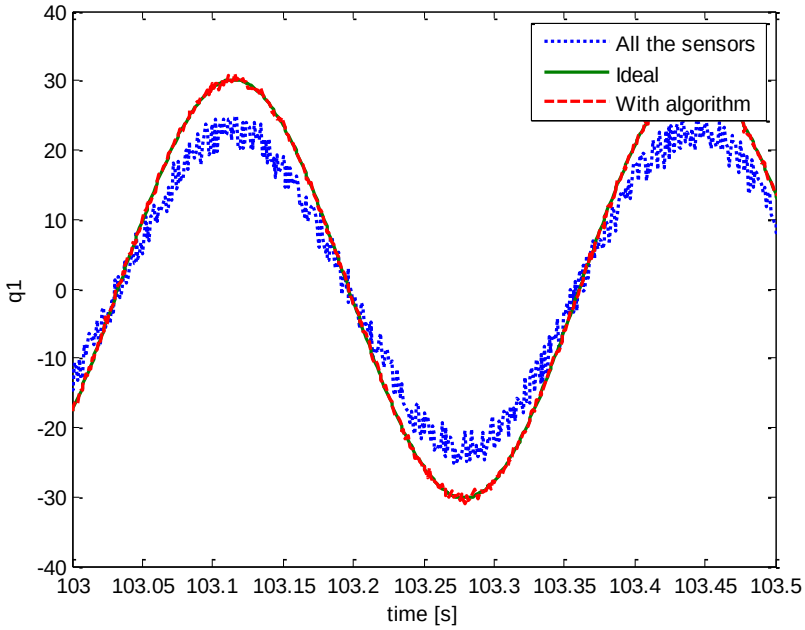

Figure 5: Sinusoidal disturbance on the first natural frequency: estimation of the first modal coordinate with and without the application of the identification algorithm.

	All the sensors	**Without faulty**
Mode 1	4.90	0.37
Mode 2	1.45	0.21
Mode 3	0.49	0.09

Table 1: RMS of the modal coordinate estimation error applying a sinusoidal disturbance on the first natural frequency.

The second test has been performed including the same sensor faults and forcing the system on the second resonance (18.3 Hz). The results of this second test are reported in figure 6 (correlation index) and figure 7 (modal coordinate estimation before and after the application of the fault identification method). It can be noticed that the algorithm correctly identifies the fault of sensors 2,7 and 10. As for the previous case (and for the same reason), the fault of sensor 13 is not recognized, since this sensor do not have a significant contribution in the estimation of the modal coordinate. In this case, the same happens with sensor 4, since (as shown in figure 3-b) it is close to a vibration node for the second mode. Anyway, the estimation of the modal coordinate after the removal of the identified faulty sensors (2,7 and 10) is strongly improved. To confirm this statement, as for the previous test, table 2 reports the RMS of the estimation of the modal coordinates with and without the removal of the sensors identified as faulty.

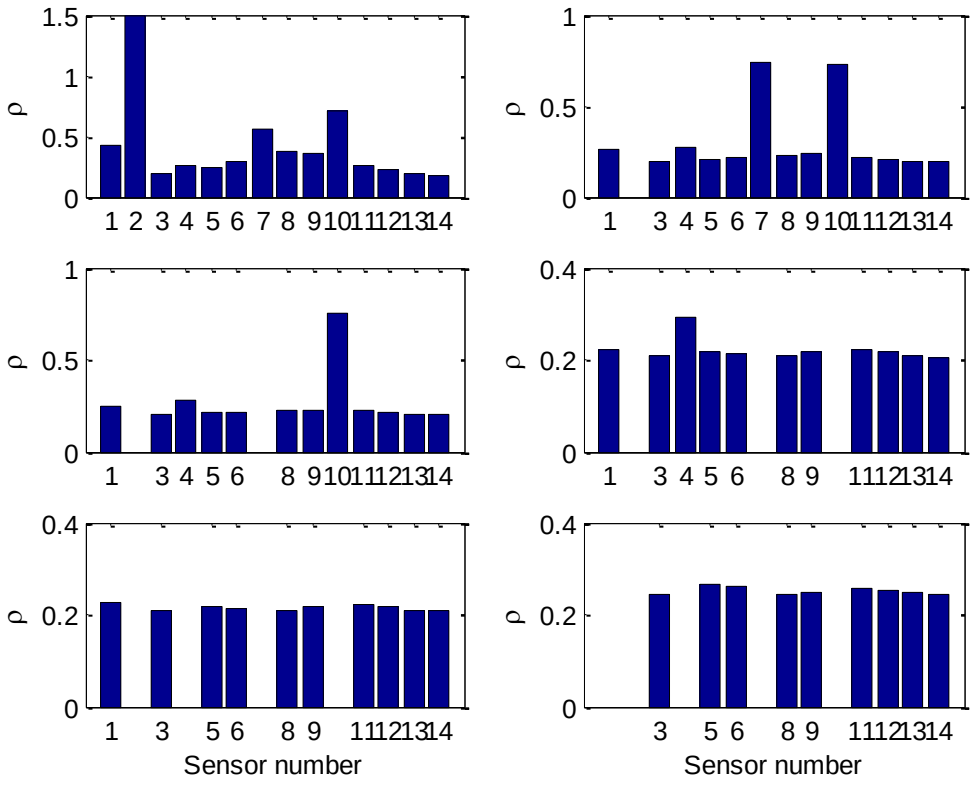

Figure 6: Sinusoidal disturbance on the second natural frequency: correlation index for the different sensors. Each figure is computed excluding the sensor identified as faulty in the previous iteration.

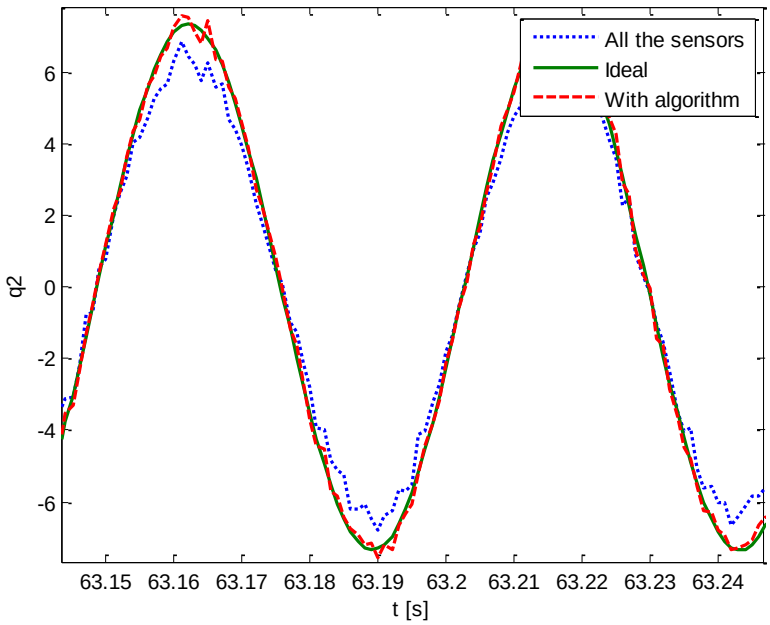

Figure 7: Sinusoidal disturbance on the second natural frequency: estimation of the second modal coordinate with and without the application of the identification algorithm.

	All the sensors	**Without faulty**
Mode 1	1.05	0.36
Mode 2	0.71	0.21
Mode 3	0.17	0.09

Table 2: RMS of the modal coordinate estimation error applying a sinusoidal disturbance on the first natural frequency.

5 CONCLUSIONS

The paper addresses the problem of the effect of damaged or faulty sensors when large arrays of sensors (such as Fiber Bragg Grating sensors) are used for vibration control. Indeed, when these sensors are applied on a structure or embedded inside it, some problems can arise, compromising the quality of the measurement and, as a consequence, the efficiency of the feedback control.
To overcome the problem, a method for the identification of faulty sensors is presented and applied to a smart structure instrumented with piezoelectric actuators and FBG sensors. This method allows identifying different types of damages and faults, strongly improving the estimation of the modal coordinates, even when multiple sensor faults are present. This result will allow to improve the performance of vibration control in case of sensor fault.

REFERENCES

[1] K. T. V. Grattan, T. Sun, Fiber optic sensor technology: an overview. *Sensors and Actuators A: Physical*, **82**(1-3), 40-61, 2000.

[2] D.R. Huston, P.L. Fuhr, J.G. Beliveau, W.B. Spillman, Structural member vibration measurements using a fiber optic sensor. *Journal of Sound Vibration*, **149**, 348-353, 1991.

[3] K. Chau, B. Moslehi, G. Song, V. Sethi, Experimental demonstration of Fiber Bragg Grating strain sensors for structural vibration control, *Proceedings of SPIE*, **5391**, 753-764, 2004.

[4] L. Cheng, Y. Zhou, M.M. Zhang, Controlled vortex-induced vibration on a fix-supported flexible cylinder in cross-flow. *Journal of Sound and Vibration*, **292**(1-2), 279-299, 2006.

[5] C. Ambrosino, G. Diodati, A. Laudati, A. Gianvito, A. Concilio, A. Sorrentino, G. Breglio, A. Cutolo, A. Cusano, Active vibration control using fiber Bragg grating sensors and piezoelectric actuators in co-located configuration. *Proceedings of SPIE*, **6619**, 2007.

[6] G. Cazzulani, S. Cinquemani, L. Comolli, F. Resta, A quasi-modal approach to overcome FBG limitations in vibration control of smart structures. *Smart Materials and Structures*, **22**(12), 2006.

[7] G. Cazzulani, S. Cinquemani, L. Comolli, A. Gardella, F. Resta, Vibration control of

smart structures using an array of Fiber Bragg Grating sensors. *Mechatronics*, **20**(4), 345-353, 2014.

[8] G. Cazzulani, S. Cinquemani, L. Comolli, A technique to evaluate the good operation of FBG sensors embedded in a carbon fiber beam. *Proceedings of SPIE*, **8794**, 2013.

[9] M. Abdelghani, M.I. Friswell, Sensor validation for structural systems with multiplicative sensor faults. *Mechanical Systems and Signal Processing*, **21**(1), 270-279, 2007.

[10] Q. Zhang, New residual generation and evaluation method for detection and isolation of faults in non-linear systems. *Journal of Adaptive Control and Signal Processing*, **14**(7), 759-773, 2000.